Waste and Biomass Valorization (2022) 13:2637–2649
https://doi.org/10.1007/s12649-022-01677-1

ORIGINAL PAPER

Synthesis of Pure Magnesium Aluminate Spinel ($MgAl_2O_4$) from Waste Aluminum Dross

Ahmed Benkhelif[1,2] · **Mostafa Kolli**[1,2]

Received: 1 June 2021 / Accepted: 3 January 2022 / Published online: 9 January 2022

Abstract

The aim of this work was the production of pure spinel ($MgAl_2O_4$) powder from waste aluminum dross by a leaching-precipitation-calcination process. The leaching treatment carried out in sulfuric acid (H_2SO_4) showed that the best leaching occurred at an acid concentration of C = 15% and a duration of 2 h at a temperature of T = 80 °C. The recovery efficiencies recorded for alumina and magnesia were 84.82% and 51.43%, respectively. The addition of 8 wt% of magnesium oxide (MgO) to the leaching solution, the precipitation with NH_4OH and the subsequent calcination at 1450 °C leads to an almost complete spinellization (> 98 wt%). The synthesized powders were pressed then sintered at 1500, 1600 and 1700 °C to elaborate compact discs. The increase in sintering temperature led to the grain growth (D15 ≈ µm at T = 1500 °C, D ≈ 35 µm at T = 1600 °C and D ≈ 70 µm at 1700 °C) and notable improvement of the density (83% at T = 1500 °C, 90% at T = 1600 °C and 93% at T = 1700 °C). The Vickers hardness (HV) and the elastic modulus (E) increased with increasing sintering temperature. The Vickers hardness reached a value of HV = 22 GPa and the elastic modulus a value of E = 220 GPa by sintering at T = 1700 °C. This increase in mechanical properties is attributed to the simultaneous effect of better consolidation and notable decrease in the total porosity (17% at 1500 °C and 7% at 1700 °C).

Graphical Abstract

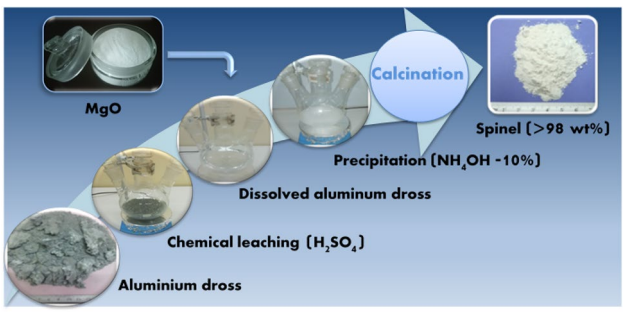

Keywords Spinel · Aluminum dross · Leaching · Alumina · Sintering

Statement of Novelty

The aluminum melting industries generate important amounts of aluminum dross that can be harmful for environment and human. This work aims to valorize these waste aluminum dross to produce a very interesting ceramic material (alumina magnesia spinel). A fine spinel ($MgAl_2O_4$) powder with a purity exceeding 98 wt% was prepared at a relatively low calcination temperature. It is expected that produced

✉ Mostafa Kolli
kolmus_eulma@yahoo.fr

[1] Emergent Materials Research Unit, Ferhat Abbas Setif 1 University, 19000 Sétif, Algeria

[2] Institute of Optics and Precision Mechanics, Ferhat Abbas Setif 1 University, 19000 Sétif, Algeria

spinel is less expensive due to the low cost of the used starting materials and the simplicity of the followed route.

Introduction

Magnesium aluminate spinel ($MgAl_2O_4$) is an excellent structural ceramic of great technological importance [1]. It has many attractive properties such as: high melting point (2135 °C), very high hardness (16 GPa), relatively low density (3.58 g/cm^3), high resistance against chemical corrosion, high thermal shock resistance, low thermal expansion coefficient [2] and an optical transmission that starts from the UV to the IR region of the electromagnetic wave spectrum (0.2–5.5 µm) [3]. These features make the use of spinel very desired in several technical and industrial applications such as refractory material, high temperature and erosion resistant windows, optical windows for pressure vessels [4, 5].

To prepare $MgAl_2O_4$ spinel, several routes can be considered. Considerations of affordability and versatility of a route stiller main as a major challenge for the materials scientists involved in the development of synthetic routes [6]. Conventionally, $MgAl_2O_4$ spinel can be prepared by sintering mixtures of MgO and Al_2O_3 powders. However, this route involves high temperatures that can exceed T = 1600 °C [7, 8]. There are also other more complex techniques, such as sol–gel [6, 9, 10], hydrolytic co-precipitation [11–13] thermal decomposition [14], combustion [15, 16], freeze drying of sulfate solutions, controlled hydrolysis of metalalkoxyde, and decomposition of organometallic compounds in supercritical fluids [17].

All over the world, the aluminum melting industries generate important quantities of aluminum dross that is mainly constituted of alumina (Al_2O_3). They may contain, also, other chemical compounds such as: $MgAl_2O_4$, AlN, Al_4C_3, MgF_2, $NaAlCl_4$, $KAlCl_4$, $Al(OH)_3$, Al_2S_3, NaCl, KCl, $FeSO_3$, SiO_2, MgO [3, 4, 18–20]. Some chemicals (AlN, Al_4C_3, Al_2S…) are very dangerous and harmful for the environment and the human being because they can react with the surrounding humidity and generate dangerous and toxic gases (H_2, CH_4, NH_3, H_2S…) [21]. During the last decades, several research works were carried out on the valorization of aluminum dross [22]. It was demonstrated the possibility of their use to synthesize high purity η-alumina and γ-alumina [23, 24], aluminum sulphate, calcium aluminates and to make refractory materials [25–27] and active catalyst [28]. Aluminum dross was, also, used to elaborate spinel composites [29, 30] and only few research studies have been devoted to the synthesis of spinel ($MgAl_2O_4$). Li et al. [30] used the aluminum dross to synthesize spinel ($MgAl_2O_4$) according to the traditional solid phase sintering. The salts contained in aluminum dross were first removed by washing in water. Subsequent heating by induction to the optimal temperature (T = 1400 °C) led to the main phases: spinel and Al_2O_3 with a purity lower than 80 wt%. The remaining impurities were found to be: SiO_2, CaO, Na_2O, and Fe_2O_3. Zhang et al. [2] elaborated spinel ($MgAl_2O_4$) by adding magnesium oxide to the unsolved part of aluminum dross leached with a basic NaOH solution. The mixture was compressed then sintered in air for 3 h between 1100 and 1500 °C. The sintering temperature T = 1400 °C was found favorable to form a spinel crystalline phase ($MgAl_2O_4$) with a purity close to 70 wt%.

In a recent work, Nguyen et al. [31] synthesized pure spinel according to two distinct methods. The first one consists of a mechanical activation by ball milling of a mixture of commercial hydro magnesite $Mg_5(CO_3)_4(OH)_2$ $4H_2O$ and alumina extracted from Aluminum dross. Complete conversion to pure spinel was reached at calcination temperature T = 1500 °C. The second method was carried out in two steps: (1) Synthesis of pure aluminum hydroxide powders by leaching in NaOH solution and precipitation by hydrogen peroxide to produce pure aluminum hydroxide powder. (2) Leaching of the resulted aluminum hydroxide powder in aqua regia and adding of MgO powder to the leaching solution then precipitation by NH_4OH solution. Complete conversion to pure spinel was achieved by calcination at 1000 °C for 5 h as was demonstrated by XRD tests. Among the two investigated methods, Co-precipitation was found to be more efficient for the synthesis of magnesium aluminate spinel. For this reason, Nguyen et al. [32] continued their research on this method and published a new work. The process used consisted of: (1) NaOH leaching of the mechanically activated aluminum dross, (2) removal of silicate(IV) from the leaching solution by adsorption followed by coagulation, (3) precipitation of pure aluminum hydroxide from the purified leaching solution, (4) dissolution of obtained aluminum hydroxide powder in aqua regia and adding of MgO powder to the leaching solution (5) precipitation by NH_4OH solution. At the end of this long method, a pure magnesium spinel (≈ 99.99%) was obtained by calcination at 1000 °C for 5 h. However, the recovery percentage of alumina in the first stage of this process did not exceed 34%.

In fact, the criteria for choosing a spinel synthesis method from aluminum dross are mainly: (1) The purity of the spinel produced, the easiness and fastness of the method that affect the product cost. (2) The recovery efficiency of Al_2O_3 and MgO since the sources of aluminum dross are limited. Some works on the synthesis of $MgAl_2O_4$ spinel neglect the use of the MgO initially contained in the dross, which significantly affects the recovery efficiency. Some other works, which conserve the MgO of the dross, produce a spinel with a low purity. In this work, we proceeded to the simultaneous recovering of alumina and magnesia by a relatively fast and uncomplicated process that consists of three main steps: leaching-precipitation-calcination. The formation of pure

spinel from the dross containing more alumina requires the addition of MgO to ensure an Al_2O_3/MgO molar ratio equal to one. For this purpose, we have firstly optimized the most important conditions of leaching by H_2SO_4 to recover the maximum possible amount of Al_2O_3 and MgO from aluminum dross. Then, we adjusted the quantity of magnesium oxide (MgO) to be added to the leaching solution and the sintering temperature necessary to achieve the complete spinellization of the precipitated powders. The synthesized spinel was characterized then shaped by uniaxial pressing in the form of discs and sintered between 1500 and 1700 °C. The properties of the elaborated spinel discs were measured and compared to the common properties of the sintered spinel.

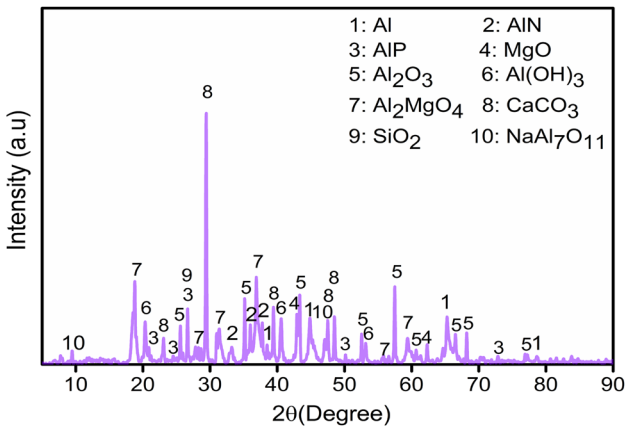

Fig. 2 X-ray diffraction pattern of the used aluminum dross

Experimental Procedure

Characterization of the Used Aluminum Dross

The aluminum dross used in this work was recovered from the production industry of aluminum profiles (AMR Company, El-Eulma—Setif industrial zone, Algeria). During the aluminum melting, aluminum dross rises to the surface of the melted aluminum bath and forms a more or less thick layer which can be extracted outside by squeegees (Fig. 1a). It is in the form of a mixture of fine powder and heavy masses of a few centimeters in size having a clear gray color (Fig. 1b). The chemical analysis of the crushed dross was carried out by XRF using an X-ray spectrometer (Rigaku Primus, IV type). This analysis was supplemented by X-ray diffraction tests (XRD) to identify all existing crystalline phases (XPERT PRO, Philips type). The amounts of these phases were determined by the semi-quantitative method using the High score plus software. The obtained XRD pattern of the aluminum dross is shown in Fig. 2, while the results of the chemical and crystallographic quantification are presented in Tables 1 and 2, respectively.

According to the literature [24, 33–36], the chemical composition of aluminum dross can vary within very large limits. Alumina content can range from 44% to more than 87%. In fact, the composition of the aluminum dross depends significantly on the composition of the molten aluminum alloy from which it is extracted. In the aluminum dross used in this work, the amount of aluminum oxide was found close to 56.5%. From a crystallographic point of view, the major current phases are aluminum in the metallic or oxide form, spinel ($MgAl_2O_4$) and calcite ($CaCO_3$).

In many research works [25, 37–42] and before being used, aluminum dross is washed with water. This allows dissolving the KCl and NaCl salts and decomposing the aluminum Nitrate (AlN) and the aluminum phosphate (AlP) according to the two following reactions [43]:

$$2AlN + 3H_2O \rightarrow Al_2O_3 + 2NH_3(g) \quad (1)$$

$$2AlP + 3H_2O \rightarrow Al_2O_3 + 2PH_3(g) \quad (2)$$

The release of the two toxic gases, ammonia (NH_3) and phosphine (PH_3), will help to secure the storage or the use of this treated dross in other purposes [43]. The washing operation allows, also, increasing the alumina amount in the washed dross, which is advantageous especially if we want to recover it. In this work and after washing of the

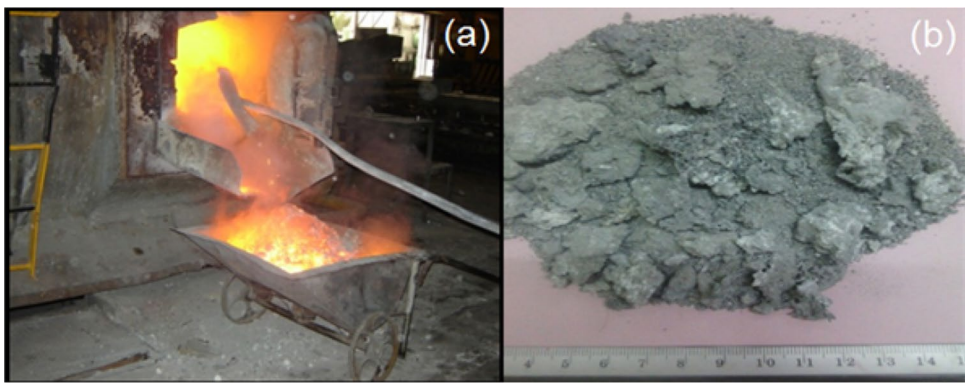

Fig. 1 Extraction of aluminum dross from the melting furnace (**a**), and the extracted raw aggregates (**b**)

Table 1 Mean chemical composition of the used aluminum dross (wt%)

Al_2O_3	CaO	MgO	SiO_2	Na_2O	P_2O_5	Cl	SO_3	Fe_2O_3	TiO_2	K_2O
56.5	11.5	12.9	6.1	4.37	2.8	2	1.0	2.05	0.8	0.6

Table 2 Crystallographic composition of the used aluminum dross

Phase	wt%
1. Aluminum, Al	7
2. Aluminum nitride, AlN	5
3. Aluminum phosphide, AlP	4
4. Magnesia, MgO	6
5. α-Al_2O_3	25
6. Aluminum hydroxide, $Al(OH)_3$	8
7. Spinel, $MgAl_2O_4$	20
8. Calcite, $CaCO_3$	16
9. Quartz, SiO_2	6
10. β-Al_2O_3 ($NaAl_7O_{11}$)	3

used dross, we recorded a significant increase in the alumina amount, which could reach 67.5% in weight instead of 56.5% before washing.

Aluminum Dross Leaching

The dross leaching was carried out in sulfuric acid (H_2SO_4) according to the protocol used by Dash et al. [44]. The tests were carried out in a three-neck flask placed on a hot plate fitted with a magnetic stirrer. We put a quantity of 10 g of the washed dross in 100 ml of sulfuric acid solution (H_2SO_4) of different concentrations (5–40%). The temperature of the solution was varied between 20 and 110 °C and the duration of leaching between 0.5 and 3 h. The obtained solution was filtered using filter paper with an opening equal to 0.2 µm. The pH of the passing solution was adjusted to pH 9 by adding ammonium hydroxide solution (NH_4OH-10%) which allows the precipitation of fine particles.

Spinellization of Aluminum Dross

To achieve complete spinellization of the precipitated particles, magnesium oxide powder (Sigma Aldrich—purity > 98%) was added to the leaching solution, in different amounts: 4, 6 and 8 wt% with respect to the initial mass of the used dross (m = 10 g). The temperature of the solution was kept equal to 50 ± 1 °C and the pH was brought to pH 9 by adding ammonium hydroxide solution (NH_4OH-10%). The precipitated particles were washed with distilled water, dried in the stove at 80 °C for 24 h and finally calcined between 1100 and 1450 °C for 2 h in a muffle furnace in air.

The synthesized powder was subjected to X-ray diffraction tests (XRD) to identify the formed phases (XPERT PRO, Philips type). The crystallite size (d) has been calculated from the XRD spectra by Scherrer's law [14]:

$$d_{RX} = K\lambda/\beta\cos\theta \quad (3)$$

K: form factor (~ 0.89); λ: wavelength of the X-rays used ($\lambda = 0.15406$ nm); β: Full width at half maximum (FWHM) of the most intense peak; θ: Bragg angle of the considered peak.

The particle size characterization of the spinel synthetized powder was carried out by laser diffraction particle size analyzer (LA-960, HORIBA) and the distilled water was used as a dispersing agent. The synthesized spinel powder was analysed and examined by X-ray spectrometer (Rigaku Primus, IV type) and scanning electron microscope (JEOL type-JSM-7001F).

Sintering of the Synthesized Spinel Powder

The spinel powder was formed into discs (D = 10 mm) by uniaxial pressing (P = 100 MPa). The sintering of the shaped discs was carried out at different temperatures (1500 °C, 1600 °C and 1700 °C) for 5 h. The physical and mechanical properties of sintered discs were monitored as a function of the sintering temperature.

The apparent density and the total porosity of the sintered spinel were measured by Arthur's method while the Vickers hardness and the elastic modulus were measured by instrumented micro-indentation tests (Zwick ZHU 2.5 KN instrumented hardness tester). The microscopic observations of the elaborated discs were carried out by a confocal microscope (Leica—DC M8 type).

Results and Discussion

Precipitates Thermal Behavior

The aluminum dross was leached in H_2SO_4 acid solution (C = 15%) for 2 h at 80 °C. Precipitates obtained after the addition of NH_4OH (10%) to the leaching solution were subjected to DT/TG analysis. The obtained curves were presented in Fig. 3. The DT/TG analyses were completed by XRD tests to follow the phase transformation of the precipitates. Figure 4 shows the XRD patterns respectively after drying at 80 °C and after calcination at different temperatures.

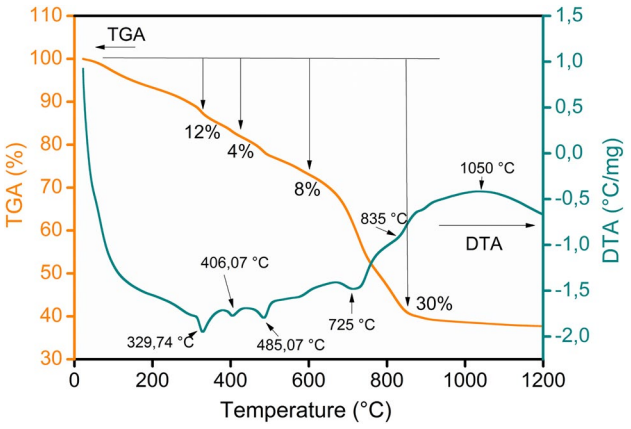

Fig. 3 DTA/TGA curves of the precipitates

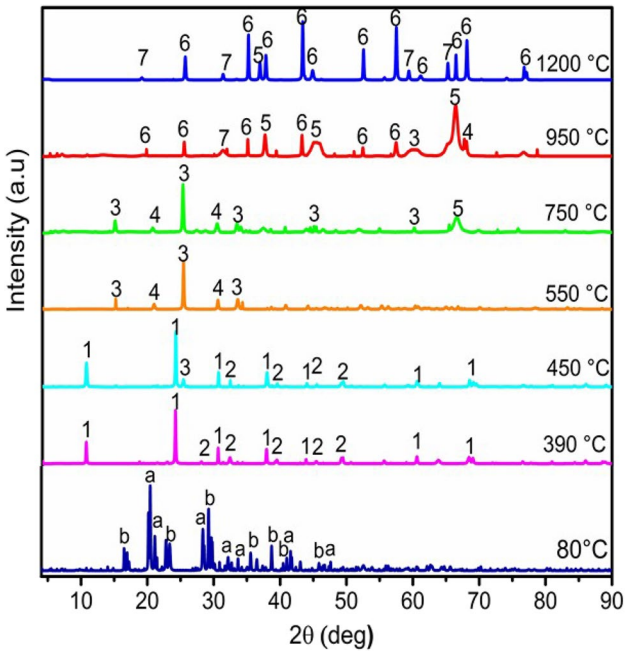

Fig. 4 XRD spectra of precipitated powder, calcined at different temperatures: a: $NH_4Al(SO_4)_2{\cdot}4H_2O$, b: $(NH_4)_2\ Mg(SO_4)_2{\cdot}6H_2O$,**1:** $NH_4Al(SO_4)_2$, **2:** $Mg_2(NH_4)_2(SO_4)_3$, **3:** $Al_2(SO_4)_3$, **4:** $MgSO_4$, **5:** $Al_{2.4}Mg_{0.4}O_4$, **6:** Al_2O_3, **7:** Al_2MgO_4

According to DTA/TGA results (Fig. 3), there is a first endothermic peak around T = 330 °C which is accompanied by a total mass loss of about 12%. This mass loss is mainly attributed to the release of bonded water from ammonium aluminum sulfate $NH_4Al(SO_4)_2{\cdot}4H_2O$ [45, 46] and ammonium hydrated magnesium sulfate $(NH_4)_2\ Mg(SO_4)_2{\cdot}6H_2O$ [47] such as suggested by XRD results presented in Fig. 4. At approximately T = 405 °C, we note a weak endothermic peak with an imperceptible mass loss (≈ 4%) which corresponds to the beginning of the decomposition of aluminum sulfate hydrated ammonium $NH_4Al(SO_4)_2$ on aluminum sulfate $Al_2(SO_4)_3$ as can be seen in the XRD spectrum (Fig. 4). At 485.07 °C, a third endothermic peak with a mass loss of about 8% was observed. It is attributed to the total decomposition of $Mg_2(NH_4)_2(SO_4)_3$ [46, 48] leading to the formation of magnesium sulfate ($MgSO_4$) as supported by XRD results. A fourth endothermic peak was observed at 719.42 °C followed by another less intense at 835 °C with a mass loss of about 30%. According to Shahbazi et al. [49] the most sulphates can be decomposed in the temperature range 719–844 °C [50]. In the obtained precipitates, the decomposition of $Al_2(SO_4)_3$ and $MgSO_4$ gives rise to the appearance of transition alumina [45, 49] and stoichiometric and non-stoichiometric spinel (Al_2MgO_4, $Al_{2.4}Mg_{0.4}O_4$). The last large exothermic peak at 1050 °C, without mass loss, corresponds to the full crystallization of the two stable phases: spinel (Al_2MgO_4) and alumina (α-Al_2O_3), as shown in the XRD pattern (Fig. 4). In the rest of this work and to ensure the completion of reactions the temperature T = 1200 °C was adopted for the precipitates calcination.

Optimization of the Leaching Stage

During the sulphuric acid leaching process, the main reactions taking place can be schematised as follow [24, 51–53]:

$$Al_2O_3 + 3H_2SO_4 \rightarrow Al_2\left(SO_4\right)_3 + 3H_2O \quad (4)$$

$$2Al + 3H_2SO_4 \rightarrow Al_2\left(SO_4\right)_3 + 3H_2(g) \quad (5)$$

$$MgAl_2O_4 + 4H_2SO_4 \rightarrow Al_2\left(SO_4\right)_3 + MgSO_4 + 4H_2O \quad (6)$$

$$MgO + H_2SO_4 \rightarrow MgSO_4 + H_2O \quad (7)$$

$$2Al(OH)_3 + 3H_2SO_4 \rightarrow Al_2\left(SO_4\right)_3 + 6H_2O \quad (8)$$

Figure 5 shows the amounts of aluminum and magnesium oxides in the synthesized powder as a function of the concentration of the H_2SO_4 acid solution for a leaching during 2 h at the temperature T = 80 °C. It is very clear that the amount of the two oxides increases significantly with the sulfuric acid concentration and reached a plateau (Al_2O_3 ≈ 86.16%, MgO ≈ 12.02%) from the concentration C = 15%. This is due to the fact that reaction products such as aluminum sulfates exerts shielding effect on the diffusion of H_2SO_4 to the dross particles and affects the reaction process. So, from some acid concentration the shielding effect of the reaction becomes more predominant than dissolution and the increase in the concentration becomes practically useless. In addition, an increase in sulfuric acid concentration induces a decrease in the fluidity of the reaction solution,

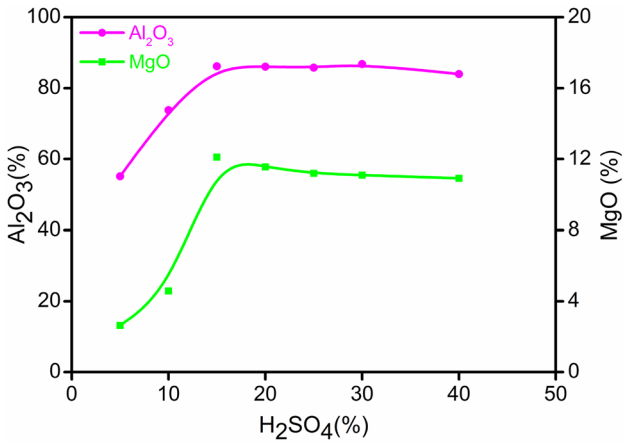

Fig. 5 Alumina and magnesium oxide amounts in the synthesized powder as a function of the concentration of H_2SO_4 acid (t = 2 h, T = 80 °C)

which can reduce the reaction rate [54]. In several research works [24, 25, 28, 44, 45], it was found that extraction of alumina from aluminum dross by leaching with H_2SO_4 acid solution increases with acid concentration and reached its maximum value at a concentration similar to that mentioned in this work (C = 15%).

The amount of the two oxides (MgO, Al_2O_3) in the synthesized powder increases over time (Fig. 6) and tends to a plateau after 2 h ($Al_2O_3 \approx 86.16\%$, MgO ≈ 12.02%).We believe that dissolution kinetics of the two oxides is completed after 2 h. According to the work of Dash et al. [44], in the first 10–15 min the reaction is very fast. After that, the reaction kinetics will be delayed due to the formation of an aluminum sulfate layer on the aluminum dross particles. After 60 min, dissolution becomes almost negligible, resulting in a constant rate of alumina recovery. Aluminum dross leaching can be thermally activated and the test temperature will significantly affects the reaction result [25, 50].

For a concentration of H_2SO_4 acid solution equal to C = 15% and a treatment time of 2 h, the amounts of alumina and magnesium oxides increase according to the solution temperature (Fig. 7). This can be brought about by the enhancement of H^+ ion activity resulting in a faster dissolution rate and a higher efficiency [55]. The amounts of alumina and magnesium oxides reach the highest values at 80 °C. Beyond this temperature, the amounts of these two oxides receive no significant increase.

Alumina and magnesia dissolution rates (R_{Al} and R_{Mg}) calculated according to the following relationships (Eqs. 9 and 10), were evaluated over time for acid concentration (C = 15%) and leaching temperature (T = 80 °C):

$$R_{Al}(\%) = \frac{Q_{Al(ext.)}}{Q_{Alini.}} * 100 \quad (9)$$

$$R_{Mg}(\%) = \frac{Q_{Mg(ext.)}}{Q_{Mg(ini.)}} * 100 \quad (10)$$

$Q_{Al\ (ext.)}$ and $Q_{Mg\ (ini.)}$ are the quantities of the considered oxide in the extracted powder and in the starting aluminum dross, respectively. It may be seen from Fig. 8 that dissolution rate increases with time and reaches a plateau after 2 h of leaching ($Al_2O_3 = 84.82\%$ and MgO = 51.43%). The slowing down of the extraction efficiency is attributed to the probable formation and coverage of the surface of the dross particle by either basic aluminum sulphate $Al_6(OH)_{10}(SO_4)_4$ or aluminum sulphate ($Al_2(SO_4)_3$) as well as magnesium sulfate ($MgSO_4$) [44] and schematised in Fig. 9. The surface of aluminum dross particles is gradually covered by a newly

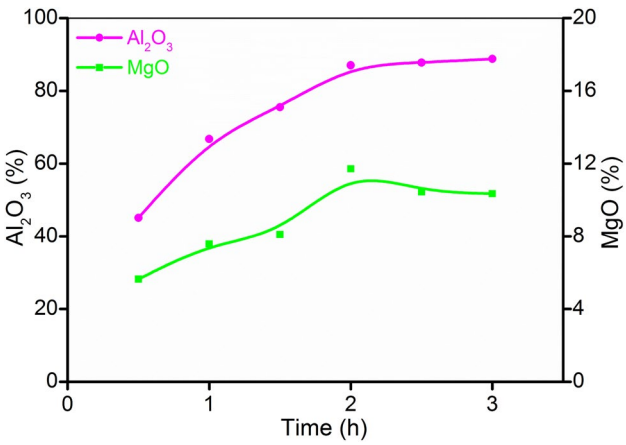

Fig. 6 Aluminum and magnesium oxides in the synthesized powder as a function of the leaching time (C = 15%, T = 80 °C)

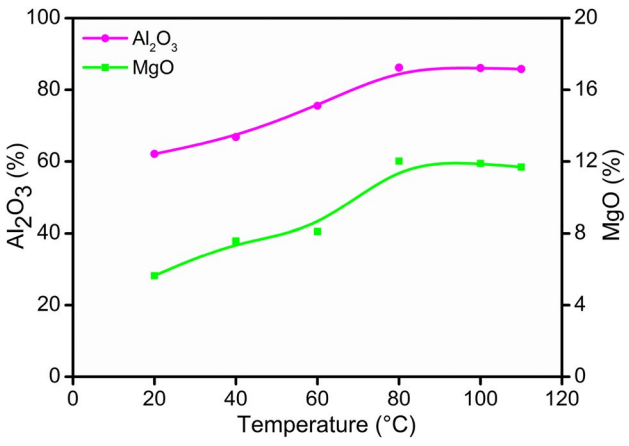

Fig. 7 Aluminum and magnesium oxides in the synthesized powder as a function of the temperature of the H_2SO_4 acid solution (C = 15%, t = 2 h)

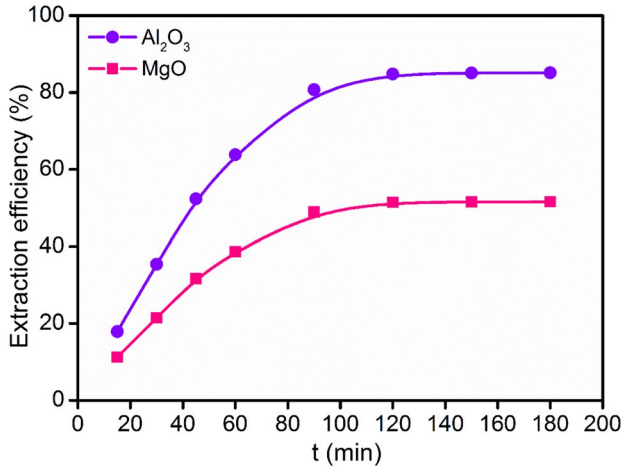

Fig. 8 Dissolution of alumina and magnesia as a function of time for acid concentration (C = 15%) and leaching temperature (T = 80 °C)

generated intermediate layer, which is so concentrated that blocks the diffusion of H_2SO_4 species considerably. Hence, for a dross particle, the dissolution process can be divided into three main stages: (1) diffusion of H_2SO_4 from solution to the external surface of dross particle, known as transitional layer diffusion: (2) diffusion of H_2SO_4 through the intermediate layer to the reaction interface: (3) chemical reaction at the interface and diffusion of metal cations into the bulk solution.

According to the obtained results, it can be concluded that a better dissolution of the aluminum dross in H_2SO_4 acid solution can be achieved with a concentration of 15% at a temperature of 80 °C for a period of 2 h. These conditions lead to an Al_2O_3/MgO mass ratio close to 7.16, which represents an insufficiency of MgO to give only a stoichiometric spinel ($MgAl_2O_4$ or $MgO{\cdot}Al_2O_3$) of a mass ratio of approximately 2.53. For this reason, the precipitates must be enriched by magnesium oxide to reach the stoichiometric composition susceptible to form spinel after calcination.

Fig. 9 Schema of the reaction between H_2SO_4 and aluminum dross particle

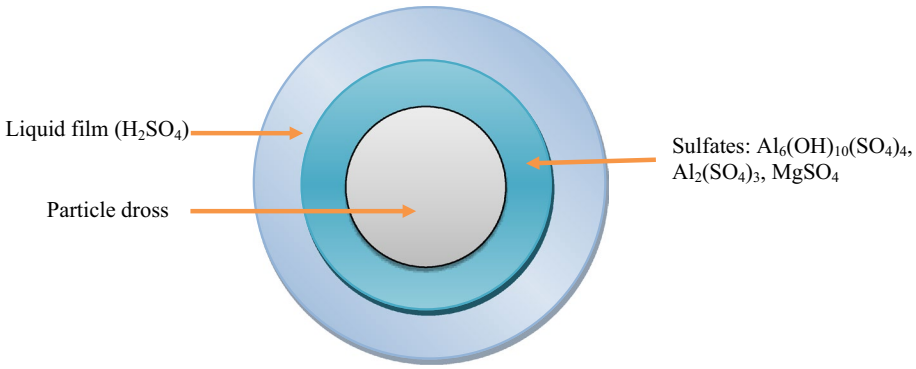

In what follows, we will present the results of the effect of adding MgO to the dissolution solution in order to achieve the complete spinellization of the Al_2O_3–MgO mixtures extracted from the aluminum dross.

Complete Spinellization of Aluminum Dross

Different amounts of MgO were previously added to the leaching solution i.e. before adding precipitation agent (NH_4OH-10%). The powders obtained after precipitation were calcined between 1100 and 1450 °C and then subjected to physico-chemical characterization.

Figures 10, 11 and 12 show the XRD spectra of the precipitates obtained by adding several magnesium oxide amounts (4, 6 and 8% in weight) and calcined at different temperatures. At the calcination temperature T = 1100 °C, three crystalline phases were identified in the precipitates, the primary spinel (Al_2MgO_4) coming from the dross,

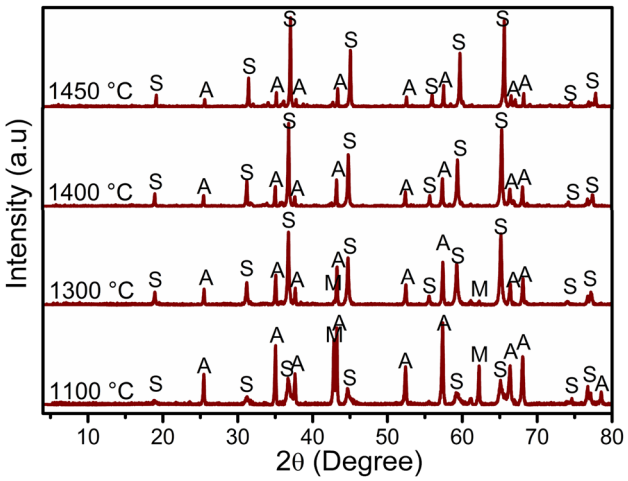

Fig. 10 XRD spectra of the precipitates calcined at different temperatures after addition of 4 wt% MgO (S = Al_2MgO_4, A = Al_2O_3, M = MgO)

alumina (Al_2O_3) and added magnesium oxide (MgO) which have not yet reacted.

With increasing calcination temperature, the added MgO reacts gradually with the alumina coming from aluminum dross and gives rise to a secondary spinel (Eq. 11). The increase in the spinel peaks intensity with calcination temperature suggests the increase in the quantity of spinel developed. For the first two additions of MgO (4 and 6%) the mass ratio Al_2O_3/MgO in the mixture (3.71 and 2.99) is far from the stoichiometric ratio of the spinel (Al_2O_3/MgO = 2.53) this is why the XRD alumina peaks persists even at T = 1450 °C.

For the third addition (MgO = 8 wt%), the stoichiometric composition of the spinel is almost respected which can lead to complete spinellization if precipitates are calcined at 1450 °C. The crystallite size for the spinel synthesized by calcination at 1450 °C calculated by Scherrer's law (Eq. 3) was found about 75 nm which is well comparable to the values found in the literature ranging from 15 to 94 nm [56, 57].

Dissolved dross **Added magnesia** **Primary spinel** **Secondary spinel**

$$MgAl_2O_4 + Al_2O_3 + MgO \rightarrow MgAl_2O_4 + MgAl_2O_4 \quad (11)$$

The purity of the synthesized spinel powder evaluated by XRF reached 98.27%. Some other oxides persist in the chemical composition with minor percentages such as CaO (0.34%), SiO_2 (0.45%), SO_3 (0.38%), Fe_2O_3 (0.3%) and Na_2O (0.26%). Zhang et al. [2] synthesized spinel ($MgAl_2O_4$) by solid-state reactions between the residues of aluminum slag and magnesium oxide. It was found that mixtures sintered at 1400 °C for 3 h contain more than 70% in mass of spinel ($MgAl_2O_4$) and exhibit a compressive strength of about 63.4 MPa.

The SEM of the synthesized spinel (Fig. 13) Show that the developed particles are in the form of agglomerates of more or less equi-axis shape. The particle size (Fig. 14) ranges from 11 nm to 2.5 µm. The average particle size is approximately equal to 550 nm which is very close to that of $MgAl_2O_4$ spinel (≈ 600 nm) synthesized by Ye et al. [58] by combining aluminum isopropoxide [Al(-O-i-C_3H_7)$_3$] and magnesium acetate tetrahydrate [$Mg(CH_3COO)_2$ $4H_2O$] in a Sol–Gel method.

The synthesized spinel can be used in the powder form in several applications for example as an additive to enhance the high temperature properties of shaped refractories [59] or castable refractories [60] and in the reinforcement of some materials [61]. In almost all cases, spinel must be formed to give dense parts by applying powder metallurgy process or sintering. Such formed spinel retrieve many applications such as refractory material (ladles and purging plugs), as a structural ceramic, and in some ballistic applications [62–66].

It's well established that sintering of spinel powders is strongly influenced by some parameters such as: powder properties (chemical composition, granulometry, additives…) and the sintering conditions (temperature, time, atmosphere, pressure) that significantly affect the diffusive phenomena taking place during sintering [67, 68]. In what

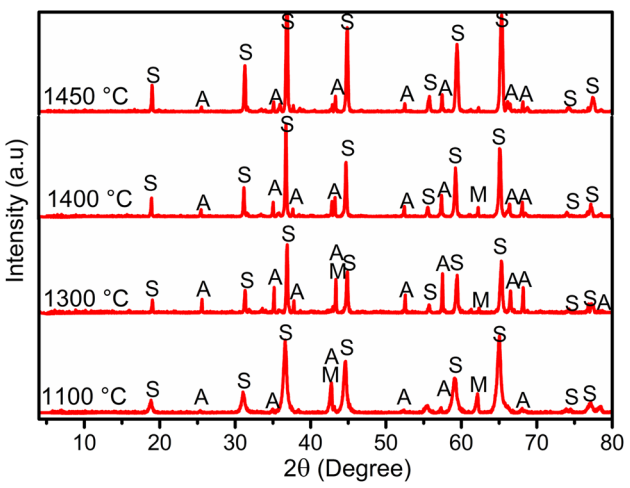

Fig. 11 XRD spectra of the precipitates calcined at different temperatures after addition of 6 wt% MgO (S = Al_2MgO_4, A = Al_2O_3, M = MgO)

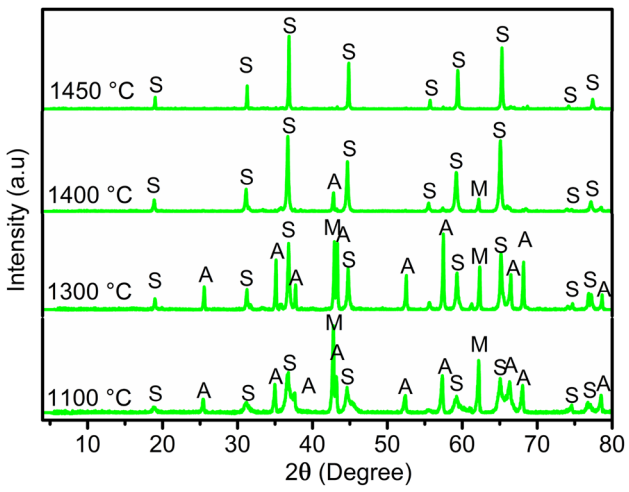

Fig. 12 XRD spectra of the precipitates calcined at different temperatures after addition of 8 wt% MgO (S = Al_2MgO_4, A = Al_2O_3, M = MgO)

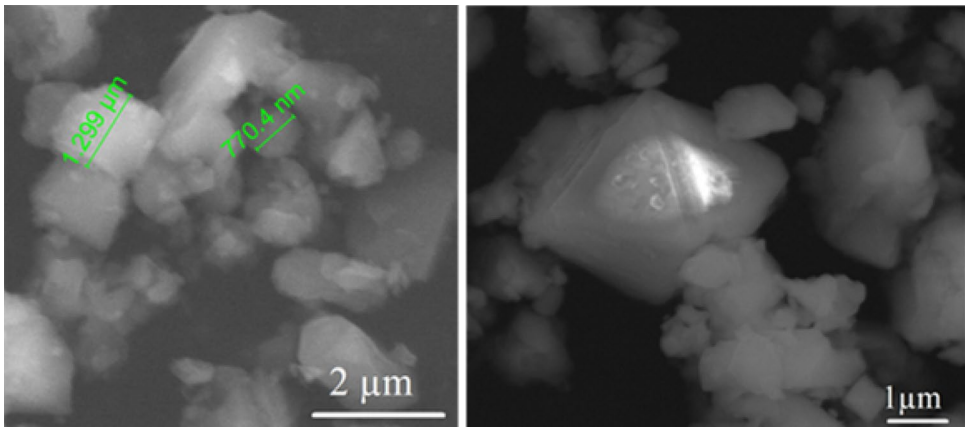

Fig. 13 SEM observation of the synthesized powder particles

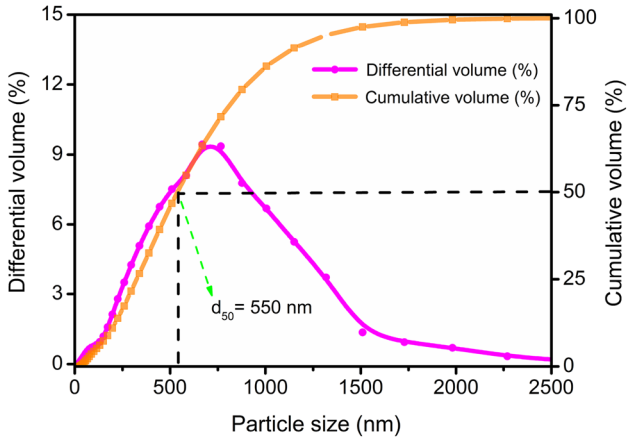

Fig. 14 Particle size distribution of the synthesized powder

follows, we investigated the effect of the most relevant sintering parameter, which is the sintering temperature on the structural and physical properties of the sintered spinel.

Sintering of the Synthesized Spinel

The synthesized spinel powder was sintered for 5 h between 1500 and 1700 °C in a free air furnace to produce compact discs. The microstructure of discs sintered at different temperatures made by confocal microscope is presented in Fig. 15.

The discs sintered at T = 1500 °C exhibit a not perfectly consolidated microstructure. There is a very large divergence in grain size that ranges from less than a micrometer to more than 15 µm. Arthur's tests method were carried out to measure the apparent density and total porosity. The apparent density measured is relatively low (83%) giving a total porosity around (17%). The observed pores (Fig. 15) are of two types: intra and inter granular and also of very different sizes [69, 70]. The increase of the sintering temperature leads to a notable reduction of the total porosity (90% at 1600 °C and 93% at 1700 °C) and grain growth (D ≈ 35 µm at T = 1600 °C and D ≈ 70 µm at 1700 °C). In the literature [71–73], it was noted that some impurities such as CaO, SiO_2 and Fe_2O_3 even with low amounts affect significantly the microstructure of sintered spinel. In this work, it seems that the unintentional presence of such impurities is responsible of the recorded densification and grain growth.

Through instrumented Vickers indentation tests, two main properties were measured on the sintered discs: Vickers hardness (HV) and elastic modulus or Young's modulus (E). The model used to calculate the elastic modulus is that developed by Oliver and Pharr [38]. The indentation load was varied between 3 and 20 N while the dwell time was kept constant for all tests carried out and equal to 15 s. Figures 16 and 17 show, respectively, the variation of the Vickers hardness and the elastic modulus according to the indentation load for all sintering temperatures. It appears that the sintering temperature influences significantly the Vickers hardness and the elastic modulus of the sintered spinel and that the indentation load has a little or no effect on the recorded values. For the indentation load P = 10 N, the spinel sintered at 1500 °C exhibits a Vickers hardness close to 13 GPa and an elastic modulus of about 90 GPa. The hardness increases to 22 GPa and the elastic modulus to E = 220 GPa by increasing sintering temperature to 1700 °C. The increase in the Vickers hardness and the elastic modulus is attributed to the better consolidation taking place in addition to the noted decrease in porosity presented in the previous section (17% at 1500 °C and 7% at 1700 °C). The Vickers hardness and elastic modulus values recorded in the current work are comparable to those found in the literature [43, 74–81]. For example, Sokol et al. [74], Ramavath et al. [75] and Maca et al. [76] found a Vickers hardness of about 13 GPa and an elastic modulus values that ranges from 279 to 288 GPa, depending on the sintering degree [74].

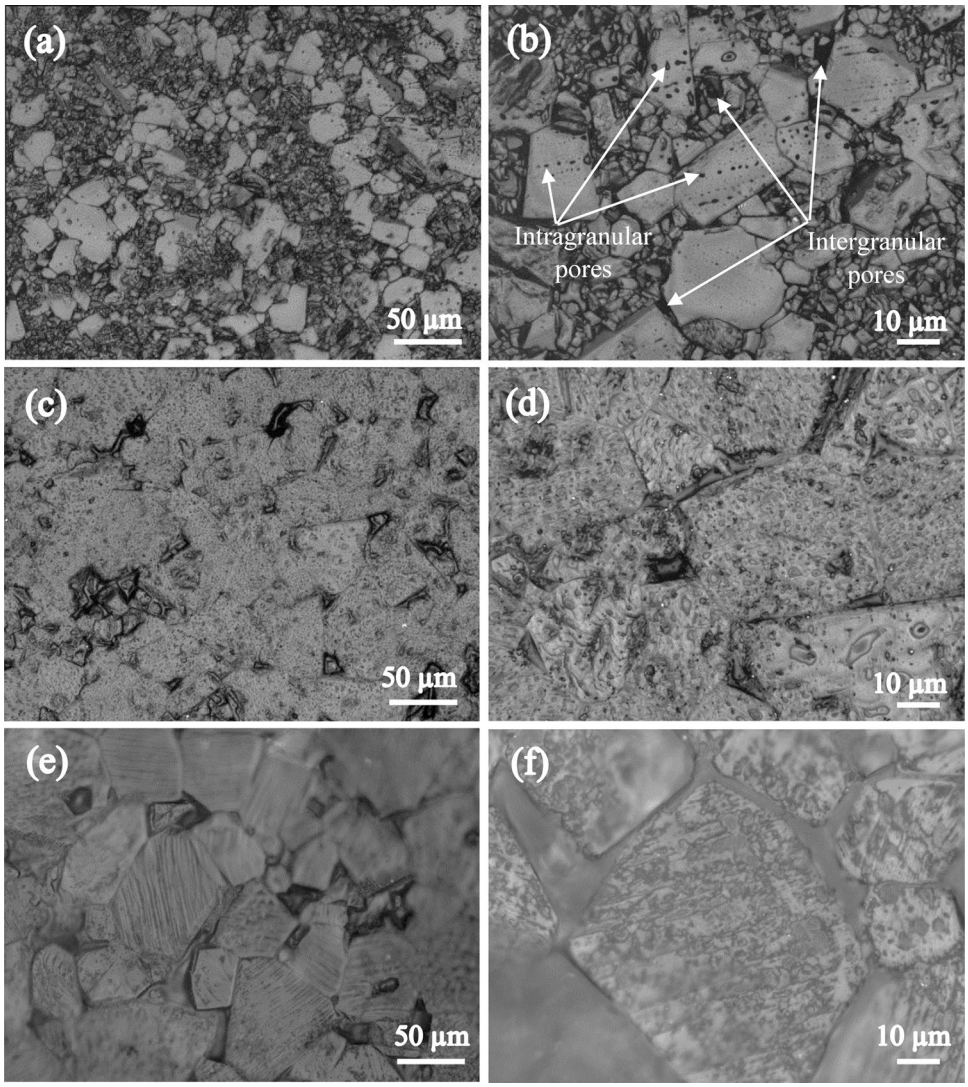

Fig. 15 Microstructure of sintered spinel sintered 5 h at different temperatures: 1500 (**a**, **b**), 1600 (**c**, **d**) and 1700 °C (**e**, **f**)

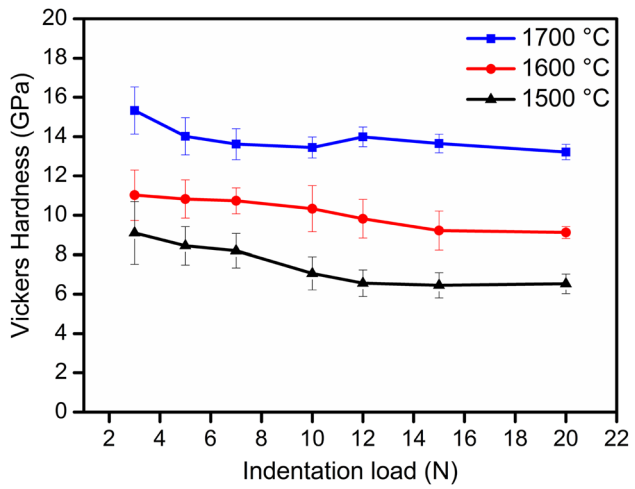

Fig. 16 Vickers hardness of syntesized spinel sintered at 1500, 1600 and 1700 °C depending on the indentation load

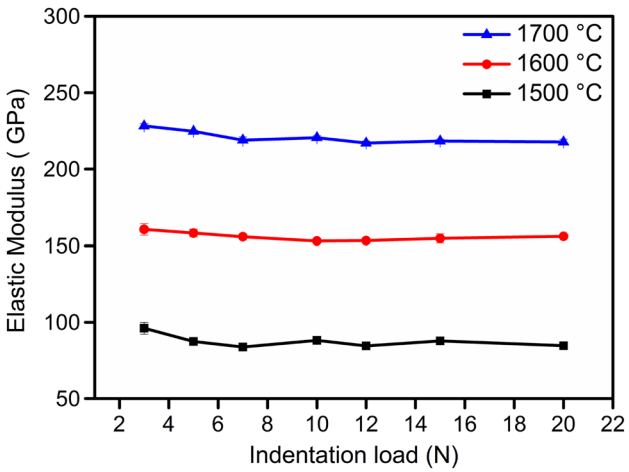

Fig. 17 Elastic modulus of the synthesized spinel sintered at 1500, 1600 and 1700 °C depending on the indentation load

Conclusion

The powders obtained after aluminum dross leaching in H_2SO_4 solution and precipitating by the NH_4OH solution (10%) undergo several microstructural transformations leading to the formation of the two stable phases: spinel (Al_2MgO_4) and α-Al_2O_3.

According to the obtained results, the optimal leaching occurs with the H_2SO_4 acid solution concentration of C = 15%, for a leaching temperature T = 80 °C and a duration of t = 2 h. Recovery efficiencies recorded for alumina and magnesia were 84.82% and 51.43%, respectively. From chemical composition point of view, the resulted precipitates consist of 86.16% in mass of Al_2O_3 and 12.02% of MgO. The addition of magnesium oxide (MgO) to the leaching solution and calcination of the precipitates at high temperature promote the reaction between free alumina and added magnesia and leads to the crystallization of a secondary spinel. The almost complete spinellization can be achieved (> 98 wt%) by addition of 8 wt% of MgO and calcination at T = 1450 °C. The developed spinel particles are in the form of agglomerates of more or less equi-axis shape of a size ranging from 11 nm to 2.5 µm and an average particle size close to 550 nm. The crystallite size was found about 75 nm.

The sintering of the synthesized spinel powders leads to a notable evolution of the microstructure that enhances significantly the density, the elastic modulus and the Vickers hardness. Sintering at 1700 °C during 5 h leads to the best results: relative density D = 93%, Vickers hardness HV = 22 GPa and elastic modulus E = 220 GPa. The spinel synthesized by this fast and easy process, which allow obtaining both high extraction efficiency and purity can be used in many industrial applications especially in the refractory sector.

Declarations

Conflict of interest The authors declare that they have no known competing financial interests or personal relationships that could have appeared to influence the work reported in this paper.

References

1. Ganesh, I., Olhero, S.M., Rebelo, A.H., Ferreira, J.M.F.: Formation and densification behavior of $MgAl_2O_4$ spinel: the influence of processing parameters. J. Am. Ceram. Soc. **91**, 1905–1911 (2008)
2. Zhang, Y., Han, Z., Xiao, X., Peng, C.: Feasibility of aluminum recovery and $MgAl_2O_4$ spinel synthesis from secondary aluminum dross. Int. J. Miner. Metall. Mater. **26**, 309–318 (2019). https://doi.org/10.1007/s12613-019-1739-3
3. Ganesh, I.: A review on magnesium aluminate ($MgAl_2O_4$) spinel: synthesis, processing and applications. Int. Mater. Rev. **58**, 63–112 (2013). https://doi.org/10.1179/1743280412Y.0000000001
4. Ganesh, I., Johnson, R., Rao, G.V.N., Mahajan, Y.R., Madavendra, S.S., Reddy, B.M.: Microwave-assisted combustion synthesis of nanocrystalline $MgAl_2O_4$ spinel powder. Ceram. Int. **31**, 67–74 (2005). https://doi.org/10.1016/j.ceramint.2004.03.036
5. Gao, L., Hong, J.S., Miyamoto, H., Torre, S.D.D.L.: Bending strength and microstructure of Al_2O_3 ceramics densified by spark plasma sintering. J. Eur. Ceram. Soc. **20**, 2149–2152 (2000). https://doi.org/10.1016/S0955-2219(00)00086-8
6. Pati, R.K., Pramanik, P.: Low-temperature chemical synthesis of nanocrystalline $MgAl_2O_4$ spinel powder. J. Am. Ceram. Soc. **83**, 1822–1824 (2000)
7. Ganesh, I.: Fabrication of magnesium aluminate ($MgAl_2O_4$) spinel foams. Ceram. Int. **37**, 2237–2245 (2011). https://doi.org/10.1016/j.ceramint.2011.03.068
8. Vitorino, N., Freitas, C., Kovalevsky, A.V., Abrantes, J.C.C., Frade, J.R.: Cellular $MgAl_2O_4$ spinels prepared by reactive sintering of emulsified suspensions. Mater. Lett. **164**, 190–193 (2016). https://doi.org/10.1016/j.matlet.2015.10.169
9. Amini, M.M., Mirzaee, M., Sepanj, N.: The effect of solution chemistry on the preparation of $MgAl_2O_4$ by hydrothermal-assisted sol–gel processing. Mater. Res. Bull. **42**, 563–570 (2007). https://doi.org/10.1016/j.materresbull.2006.06.011
10. Sanjabi, S., Obeydavi, A.: Synthesis and characterization of nanocrystalline $MgAl_2O_4$ spinel via modified sol–gel method. J. Alloys Compd. **645**, 535–540 (2015). https://doi.org/10.1016/j.jallcom.2015.05.107
11. Li, G., Sun, Z., Chen, C., Cui, X., Ren, R.: Synthesis of nanocrystalline $MgAl_2O_4$ spinel powders by a novel chemical method. Mater. Lett. **61**, 3585–3588 (2007). https://doi.org/10.1016/j.matlet.2006.11.123
12. Alvar, E.N., Rezaei, M., Alvar, H.N.: Synthesis of mesoporous nanocrystalline $MgAl_2O_4$ spinel via surfactant assisted precipitation route. Powder Technol. (2010). https://doi.org/10.1016/J.POWTEC.2009.11.019
13. Ewais, E.M.M., El-Amir, A.A.M., Besisa, D.H.A., Esmat, M., El-Anadouli, B.E.H.: Synthesis of nanocrystalline MgO/$MgAl_2O_4$ spinel powders from industrial wastes. J. Alloys Compd. **691**, 822–833 (2017). https://doi.org/10.1016/j.jallcom.2016.08.279
14. Miroliaee, A., Salehirad, A., Rezvani, A.R.: Ion-pair complex precursor approach to fabricate high surface area nanopowders of $MgAl_2O_4$ spinel. Mater. Chem. Phys. **151**, 312–317 (2015). https://doi.org/10.1016/j.matchemphys.2014.11.072
15. Ianoş, R., Lazău, R.: Combustion synthesis, characterization and sintering behavior of magnesium aluminate ($MgAl_2O_4$) powders. Mater. Chem. Phys. **115**, 645–648 (2009). https://doi.org/10.1016/j.matchemphys.2009.01.028
16. Salem, S.: Application of autoignition technique for synthesis of magnesium aluminate spinel in nano scale: influence of starting solution pH on physico-chemical characteristics of particles. Mater. Chem. Phys. **155**, 59–66 (2015). https://doi.org/10.1016/j.matchemphys.2015.01.066
17. Abdi, M.S., Ebadzadeh, T., Ghaffari, A., Feli, M.: Synthesis of nano-sized spinel ($MgAl_2O_4$) from short mechanochemically activated chloride precursors and its sintering behavior. Adv. Powder Technol. **26**, 175–179 (2015). https://doi.org/10.1016/j.apt.2014.09.011
18. Hwang, J.Y., Huang, X., Xu, Z.: Recovery of metals from aluminum dross and saltcake. J. Miner. Mater. Charact. Eng. **5**, 47–62 (2006). https://doi.org/10.4236/jmmce.2006.51003
19. Samuel, M.: A new technique for recycling aluminium scrap. J. Mater. Process. Technol. **135**, 117–124 (2003). https://doi.org/10.1016/S0924-0136(02)01133-0
20. Bajare, D., Berzina-Cimdina, L., Stunda, A., Rozenstrauha, I., Korjakins, A.: Characterisation and application of the mix of

oxides from secondary aluminium industry. In: 2nd International Congress on Ceramics (2008)
21. Gil, A., Korili, S.A.: Management and valorization of aluminum saline slags: current status and future trends. Chem. Eng. J. **289**, 74–84 (2016). https://doi.org/10.1016/j.cej.2015.12.069
22. Meshram, A., Singh, K.K.: Recovery of valuable products from hazardous aluminum dross: a review. Resour. Conserv. Recycl. **130**, 95–108 (2018). https://doi.org/10.1016/j.resconrec.2017.11.026
23. Das, B.R., Dash, B., Tripathy, B.C., Bhattacharya, I.N., Das, S.C.: Production of η-alumina from waste aluminium dross. Miner. Eng. **20**, 252–258 (2007). https://doi.org/10.1016/j.mineng.2006.09.002
24. How, L.F., Islam, A., Jaafar, M.S., Taufiq-Yap, Y.H.: Extraction and characterization of γ-alumina from waste aluminium dross. Waste Biomass Valoriz. **8**, 321–327 (2017)
25. David, E., Kopac, J.: Aluminum recovery as a product with high added value using aluminum hazardous waste. J. Hazard. Mater. **261**, 316–324 (2013). https://doi.org/10.1016/j.jhazmat.2013.07.042
26. Brisson, C., Chauvette, G., Kimmerle, F.M., Roussel, R.: Process for using dross residues to produce refractory products, US patent **5**, 132–246 (1992)
27. Adeosun, S.O., Sekunowo, O.I., Taiwo, O.O., Ayoola, W.A., Machado, A.: Physical and mechanical properties of aluminum dross. Advan. Mater. **3**, 6–10 (2014). https://doi.org/10.11648/j.am.20140302.11
28. Breault, R., Tremblay, S.P., Huard, Y., Mathieu, G.: Process for the preparation of calcium aluminates from aluminum dross residues. US patent **5**, 407–459 (1995)
29. Kim, J., Biswas, K., Jhon, K.-W., Jeong, S.-Y., Ahn, W.-S.: Synthesis of AlPO4-5 and CrAPO-5 using aluminum dross. J. Hazard. Mater. **169**, 919–925 (2009). https://doi.org/10.1016/j.jhazmat.2009.04.035
30. Li, P., Guo, M., Zhang, M., Wang, X.D., Seetharaman, S.: Spinel synthesis from aluminium dross. Miner. Process. Extr. Metall. **120**, 247–250 (2011). https://doi.org/10.1179/1743285511Y.0000000007
31. Nguyen, T.T.N., Lee, M.S.: Synthesis of magnesium aluminate spinel powder from the purified sodium hydroxide leaching solution of black dross. Processes **7**, 741 (2019)
32. Nguyen, T.T.N., Song, S.J., Lee, M.S.: Development of a hydrometallurgical process for the recovery of pure alumina from black dross and synthesis of magnesium spinel. J. Mater. Res. Technol. **9**, 2568–2577 (2020)
33. Shinzato, M.C., Hypolito, R.: Solid waste from aluminum recycling process: characterization and reuse of its economically valuable constituents. Waste Manag. **25**, 37–46 (2005)
34. Yoshimura, H.N., Abreu, A.P., Molisani, A.L., de Camargo, A.C., Portela, J.C.S., Narita, N.E.: Evaluation of aluminum dross waste as raw material for refractories. Ceram. Int. **34**, 581–591 (2008). https://doi.org/10.1016/j.ceramint.2006.12.007
35. Ewais, E.M.M., Khalil, N.M., Amin, M.S., Ahmed, Y.M.Z., Barakat, M.A.: Utilization of aluminum sludge and aluminum slag (dross) for the manufacture of calcium aluminate cement. Ceram. Int. **35**, 3381–3388 (2009). https://doi.org/10.1016/j.ceramint.2009.06.008
36. Holappa, L., Kaçar, Y.: Slag formation—thermodynamic and kinetic aspects and mechanisms. In: Reddy, R.G., Chaubal, P., Pistorius, P.C., Pal, U. (eds.) Advances in Molten Slags, Fluxes, and Salts: Proceedings of the 10th International Conference on Molten Slags, Fluxes and Salts 2016, pp. 1017–1024. Springer International Publishing, Cham (2016)
37. V. (Hrsg.), F.W. in der G.D.C. in G. mit dem N.W. (NAW) im D.D.I. für N. e: Deutsche Einheitsverfahren zur Wasser-, Abwasser-und Schlammuntersuchung, Verfahren S4: Bestimmung der Eluierbarkeit mit Wasser (DIN 38414 Teil 4). 13. (1984)
38. Pharr, G.M., Oliver, W.C.: Measurement of thin film mechanical properties using nanoindentation. MRS Bull. **17**, 28–33 (1992). https://doi.org/10.1557/S0883769400041634
39. López-Delgado, A., Tayibi, H.: Can hazardous waste become a raw material? The case study of an aluminium residue: a review. Waste Manag. Res. **30**, 474–484 (2012). https://doi.org/10.1177/0734242X11422931
40. Xiao, Y., Reuter, M.A., Boin, U.: Aluminium recycling and environmental issues of salt slag treatment. J. Environ. Sci. Health A **40**, 1861–1875 (2005). https://doi.org/10.1080/10934520500183824
41. Lorber, K.: Treatment and disposal of residues from aluminum dross recover. In: Crete 2010—2nd International Conference on Hazardous and Industrial Waste Management—Proceedings, pp. 187–188 (2010)
42. Shen, H., Forssberg, E.: An overview of recovery of metals from slags. Waste Manag. **23**, 933–949 (2003). https://doi.org/10.1016/S0956-053X(02)00164-2
43. Tsakiridis, P.E.: Aluminium salt slag characterization and utilization—a review. J. Hazard. Mater. **217–218**, 1–10 (2012). https://doi.org/10.1016/j.jhazmat.2012.03.052
44. Dash, B., Das, B.R., Tripathy, B.C., Bhattacharya, I.N., Das, S.C.: Acid dissolution of alumina from waste aluminium dross. Hydrometallurgy **92**, 48–53 (2008). https://doi.org/10.1016/j.hydromet.2008.01.006
45. Amer, A.M.: Extracting aluminum from dross tailings. JOM **54**, 72–75 (2002). https://doi.org/10.1007/BF02709754
46. Park, H.C., Park, Y.J., Stevens, R.: Synthesis of alumina from high purity alum derived from coal fly ash. Mater. Sci. Eng. A **367**, 166–170 (2004). https://doi.org/10.1016/j.msea.2003.09.093
47. Kosova, D.A., Druzhinina, A.I., Tiflova, L.A., Monayenkova, A.S., Uspenskaya, I.A.: Thermodynamic properties of ammonium magnesium sulfate hexahydrate $(NH_4)_2Mg(SO_4)_2{\cdot}6H_2O$. J. Chem. Thermodyn. **118**, 206–214 (2018). https://doi.org/10.1016/j.jct.2017.11.016
48. Wang, W., Gu, H.M., Zhai, Y.C.: Study on extraction of Mg from boron mud. Adva. Mater. Res. **881–883**, 671–674 (2014)
49. Shahbazi, H., Shokrollahi, H., Alhaji, A.: Optimizing the gel-casting parameters in synthesis of $MgAl_2O_4$ spinel. J. Alloys Compd. **712**, 732–741 (2017)
50. Sangita, S., Nayak, N., Panda, C.R.: Extraction of aluminium as aluminium sulphate from thermal power plant fly ashes. Trans. Nonferrous Met. Soc. China **27**, 2082–2089 (2017)
51. Teodorescu, R., Badilita, V., Roman, M., Purcaru, V., Capota, P., Tociu, C., Gheorghe, M., Crisan, A.: Optimization of process for total recovery of aluminum from smelting slag 2. Removal of aluminum sulfate. Environ. Eng. Manag. J. **13**, 7–14 (2013)
52. Meshram, A., Jain, A., Gautam, D., Singh, K.K.: Synthesis and characterization of tamarugite from aluminium dross: part I. J. Environ. Manag. **232**, 978–984 (2019)
53. Zhang, S., Zhu, W., Li, Q., Zhang, W., Yi, X.: Recycling of secondary aluminum dross to fabricate porous γ-Al_2O_3 assisted by corn straw as biotemplate. J. Mater. Sci. Chem. Eng. **7**, 87–102 (2019)
54. Zheng, G., Xia, J., Liu, C., Yang, J.: Kinetics of aluminum extraction from aluminum ash by leaching with sulfuric acid. Phosphorus Sulfur Silicon Relat. Elem. **195**, 536–543 (2020)
55. Mahinroosta, M., Allahverdi, A.: Enhanced alumina recovery from secondary aluminum dross for high purity nanostructured γ-alumina powder production: kinetic study. J. Environ. Manag. **212**, 278–291 (2018)
56. Schreyeck, L., Wlosik, A., Fuzellier, H.: Influence of the synthesis route on $MgAl_2O_4$ spinel properties. J. Mater. Chem. **11**, 483–486 (2001)

57. Li, J.-G., Ikegami, T., Lee, J.-H., Mori, T., Yajima, Y.: Synthesis of Mg–Al spinel powder via precipitation using ammonium bicarbonate as the precipitant. J. Eur. Ceram. Soc. **21**, 139–148 (2001)
58. Ye, G., Oprea, G., Troczynski, T.: Synthesis of $MgAl_2O_4$ spinel powder by combination of sol–gel and precipitation processes. J. Am. Ceram. Soc. **88**, 3241–3244 (2005)
59. Ganesh, I., Bhattacharjee, S., Saha, B.P., Johnson, R., Rajeshwari, K., Sengupta, R., Rao, M.R., Mahajan, Y.R.: An efficient $MgAl_2O_4$ spinel additive for improved slag erosion and penetration resistance of high-Al_2O_3 and MgO–C refractories. Ceram. Int. **28**, 245–253 (2002)
60. Wang, F., Chen, P., Li, X., Zhu, B.: Effect of micro-spinel powders addition on the microstructure and properties of alumina refractory castables. Ceram. Int. **45**, 2989–2999 (2019)
61. El-Amir, A.A., Li, S., Abdelgawad, M., Ewais, E.M.: $MgAl_2O_4$ reinforced c-ZrO_2 ceramics prepared by spark plasma sintering. J. Korean Ceram. Soc. **58**, 574–582 (2021)
62. Schmidtmeier, D., Buchel, G., Buhr, A.: Magnesium aluminate spinel raw materials for high performance refractories for steel ladles. Mater. Ceram. **61**, 223–227 (2009)
63. Braulio, M.A.L., Rigaud, M., Buhr, A., Parr, C., Pandolfelli, V.C.: Spinel-containing alumina-based refractory castables. Ceram. Int. **37**, 1705–1724 (2011)
64. Racher, R.P., McConnell, R.W., Buhr, A.: Magnesium aluminate spinel raw materials for high performance refractories for steel ladles. In: 43rd Conference of Metallurgists (2004)
65. Schnabel, M., Buhr, A., Exenberger, R., Rampitsch, C.: Spinel: in-situ versus preformed-clearing the myth. Refract. Worldforum **2**, 87–93 (2010)
66. Haney, E.J., Subhash, G.: Damage mechanisms perspective on superior ballistic performance of spinel over sapphire. Exp. Mech. **53**, 31–46 (2013)
67. Ul'yanova, A.V., Senina, M.O., Lemeshev, D.O.: Preparation of dense ceramics based on aluminum–magnesium spinel by forming solid solutions in the $MgAl_2O_4$–Ga_2O_3 system. Russ. J. Inorg. Chem. **66**, 1245–1251 (2021)
68. Shi, Z., Zhao, Q., Guo, B., Ji, T., Wang, H.: A review on processing polycrystalline magnesium aluminate spinel ($MgAl_2O_4$): sintering techniques, material properties and machinability. Mater. Des. **193**, 108858 (2020)
69. Gajdowski, C.: Élaboration de spinelle $MgAl_2O_4$ transparent par frittage naturel et post-HIP pour des applications en protections balistiques, Thèse de doctorat. Université de Valenciennes et du Hainaut-Cambresis (2018)
70. Ganesh, I., Reddy, G.J., Sundararajan, G., Olhero, S.M., Torres, P.M., Ferreira, J.M.: Influence of processing route on microstructure and mechanical properties of $MgAl_2O_4$ spinel. Ceram. Int. **36**, 473–482 (2010)
71. Kim, T., Kim, D., Kang, S.: Effect of additives on the sintering of $MgAl_2O_4$. J. Alloys Compd. **587**, 594–599 (2014)
72. Zawrah, M.F.: Investigation of lattice constant, sintering and properties of nano Mg–Al spinels. Mater. Sci. Eng. A **382**, 362–370 (2004)
73. Saleh, Q.A., Hassen, B.F.: Effect of CaO addition on the sintering behavior and microstructure of stoichiometric spinel. Int. J. Phys. **5**, 57–62 (2017)
74. Sokol, M., Kalabukhov, S., Shneck, R., Zaretsky, E., Frage, N.: Effect of grain size on the static and dynamic mechanical properties of magnesium aluminate spinel ($MgAl_2O_4$). J. Eur. Ceram. Soc. **37**, 3417–3424 (2017)
75. Ramavath, P., Biswas, P., Rajeswari, K., Suresh, M.B., Johnson, R., Padmanabham, G., Kumbhar, C.S., Chongdar, T.K., Gokhale, N.M.: Optical and mechanical properties of compaction and slip cast processed transparent polycrystalline spinel ceramics. Ceram. Int. **40**, 5575–5581 (2014)
76. Maca, K., Trunec, M., Chmelik, R.: Processing and properties of fine-grained transparent $MgAl_{\sim 2}O_{\sim 4}$ ceramics. Ceram. Silik. **51**, 94 (2007)
77. Feng, H., Fang, Q.H., Zhang, L.C., Liu, Y.W.: Special rotational deformation and grain size effect on fracture toughness of nanocrystalline materials. Int. J. Plast. **42**, 50–64 (2013)
78. Atkinson, A., Bastid, P., Liu, Q.: Mechanical properties of magnesia–spinel composites. J. Am. Ceram. Soc. **90**, 2489–2496 (2007)
79. Tricoteaux, A., Rguiti, E., Chicot, D., Boilet, L., Descamps, M., Leriche, A., Lesage, J.: Influence of porosity on the mechanical properties of microporous β-TCP bioceramics by usual and instrumented Vickers microindentation. J. Eur. Ceram. Soc. **31**, 1361–1369 (2011)
80. Asmani, M., Kermel, C., Leriche, A., Ourak, M.: Influence of porosity on Young's modulus and Poisson's ratio in alumina ceramics. J. Eur. Ceram. Soc. **21**, 1081–1086 (2001)
81. Rothman, A., Kalabukhov, S., Sverdlov, N., Dariel, M.P., Frage, N.: The effect of grain size on the mechanical and optical properties of spark plasma sintering-processed magnesium aluminate spinel Mg Al_2O_4. Int. J. Appl. Ceram. Technol. **11**, 146–153 (2014)